# Flash-boiling liquid ammonia fuel spray near supercritical transition conditions

Kaushik Nonavinakere Vinod<sup>1</sup>, William L. Roberts<sup>2</sup>, Tiegang Fang\*<sup>1</sup>

<sup>1</sup>Dept. of Mechanical and Aerospace Engineering, North Carolina State University, Raleigh, NC, USA

<sup>2</sup>Clean Combustion Research Center, King Abdullah University of Science and Technology, Thuwal, Saudi Arabia

### **Abstract**

Recent trends in decarbonizing efforts have brought ammonia to the forefront of research as a fuel for energy and transportation. But several previous studies have strongly suggested that ammonia has difficulties in ignition and heat release when used in a gaseous form due to its physical properties. On the other hand, working with liquid ammonia presents countless problems like difficulty in pressurizing, damage to elastomers and other metals, etc. In this study, pure liquid ammonia is injected into a CVCC (constant volume combustion chamber) using a hollow cone injector to understand the behavior of liquid ammonia when pressurized. Specifically, varying ambient temperature and pressure conditions encompassing the fuel's subcritical to the supercritical regimes are studied as liquid ammonia tends to rapidly vaporize and flash-boil at pressures and temperatures above 50 bar and 315 K. High-speed shadowgraph and Schlieren imaging techniques are used to characterize the spray and understand the effects of varying conditions. Based on the formation of the central plume due to collapsing spray, many measurements like the plume ratio and penetration are studied to indicate the fuel's transition into the transcritical regime. A measurement of the flash-boiling spray plume ratios along with the spray penetration data give us a correlation of the environmental conditions to the spray transitioning into the supercritical regime. Interestingly, increasing the injection pressure from 75 bar to 150 bar shows 3 distinct regimes forming in the central spray plume penetration and the sprat plume ratio. This study has novel contribution to the development of direct injection of liquid ammonia spray for applications in high-power density engine systems.

## **Keywords**

Liquid ammonia injection, Flash-boiling ammonia spray, Hollow cone spray, Supercritical ammonia spray

#### Introduction

Ammonia's potential as a future fuel is garnering significant attention and consideration for several compelling reasons. Firstly, ammonia offers an avenue for decarbonizing various sectors, particularly transportation and energy production. Its composition devoid of carbon renders it as a clean-burning fuel, making it a promising alternative to fossil fuels. As the world grapples with the challenges posed by climate change, the need for low or zero-emission energy sources has become imperative. Ammonia, with its capacity to produce zero carbon emissions when burned, stands out as a viable solution in this context [1-3]. Ammonia (NH<sub>3</sub>), recognized as a viable carrier of hydrogen, contains 17.8% hydrogen by weight and burns without emitting carbon dioxides (CO<sub>2</sub>), making it a carbon-free molecule. Notably, NH<sub>3</sub> is a safer and more easily transportable fuel, capable of liquefaction at room temperature under 8.0 bar pressure. Additionally, existing infrastructures for ammonia production, transportation, and storage support its use. Consequently, extensive research has focused on ammonia's fundamental properties and its application in combustion devices [4-6]. Lately, liquid ammonia

has gained attention due to its unique properties: a high ignition temperature and a narrow flammable range. This has led to extensive research in the realm of dual fuel combustion. Researchers have investigated high-pressure liquid ammonia spray ignition using a pilot diesel flame at pressures reaching 53 MPa. Their findings identified the significant impact of the interaction between the diesel and ammonia jets on ignition delay and heat release rates in ammonia combustion. Optical diagnostics revealed crucial insights into spray and flame characteristics [7-10], highlighting the flame instability rooted in challenges achieving an optimal fuel-air mixture quality. Ultimately, the interactions between diesel and liquid ammonia sprays and the precision of ammonia-air mixture formation are critical for achieving highly efficient ammonia combustion [11-15]. Consequently, designing predictive models for the spray characteristics of high-pressure liquefied fuel gas, particularly liquid ammonia, remains pivotal in advancing this field.

The fuel/air mixing characteristics of an ammonia spray under conditions directly relevant to engine operation remain insufficiently explored. A crucial aspect requiring investigation is the occurrence of the flash boiling phenomenon, which arises due to the distinctive physical properties of ammonia. Efforts to study flash-boiling sprays reveal correlations between macroscopic spray structure and the superheated degree of the fuel. Based on that, the spray can be categorized into non-flash boiling, transition, and flare-flash boiling regimes. Several studies investigated spray's near-field primary breakup under flash boiling, highlighting radial propagation triggered by vapor bubble explosions and collapses. They noted that the intensity of these explosions is notably influenced by the nozzle's flow regime. Additionally, injector configurations and various factors play roles in affecting flash boiling [16-19].

In summary, to utilize ammonia as potential fuel in a high-power engine system, it is necessary to understand its spray performance and injection dynamics, particularly under high injection pressure. Studies focusing on the flash-boiling phenomenon of liquid ammonia are important in developing systems that can utilize the fuel's thermophysical properties to our advantage. But there are no studies that compare the performance of the fuel under different flash-boiling conditions and different injector designs. This study aims to study the flash-boiling of liquid ammonia using an ammonia pressurization system to understand the interaction between the ambient conditions and the fuel injection properties in a constant volume combustion chamber (CVCC). It is possible to improve the performance of fuel-air mixing in engines by using flash-boiling liquid ammonia.

# **Experimental setup**

For this study, the experimental setup consists of three individual subsystems that were modified in one way or another to be compatible working with liquid ammonia. Figure 1 shows a schematic of the experimental setup used in this study. Table 1 shows selected thermophysical properties of ammonia. The individual systems used in this study are discussed in detail in the following subsections.

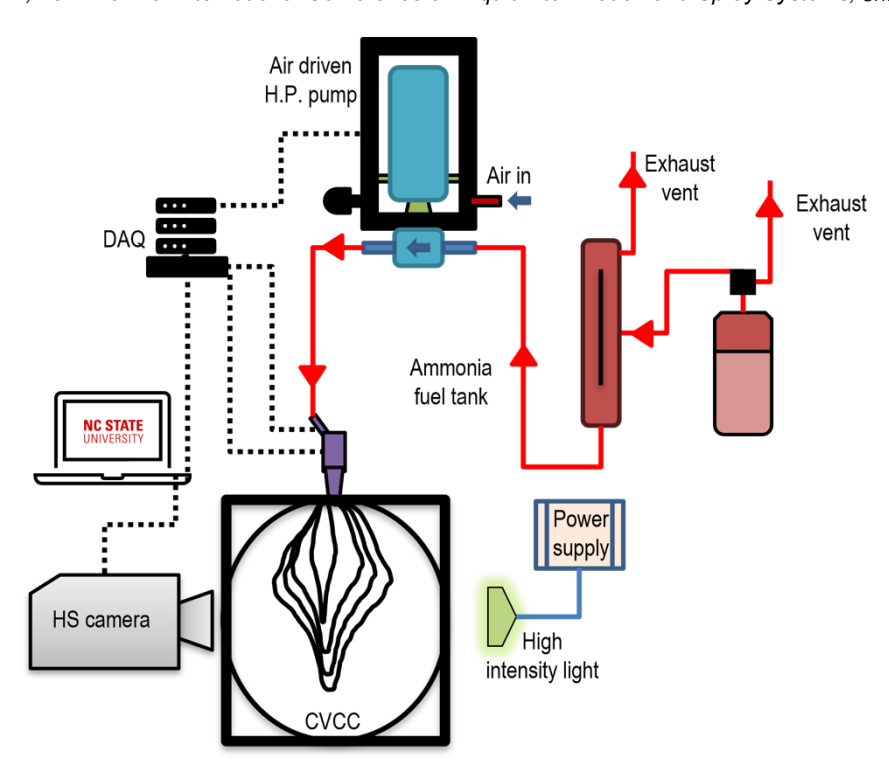


Figure 1 Schematic of the experimental setup used in this study.

Table 1 Thermophysical properties of ammonia used in this study.

Description (units)	Value	
LHV (MJ/kg)	18.73	
Adiabatic flame temperature (K)	2123	
Minimum auto-ignition temperature (K)	920	
Stoichiometric air/fuel ratio (%)	6.05	
Boiling point (K)	240	
Latent heat of vaporization @ 1 bar (kJ/kg)	1365	
Density (kg/m3)	612	
Critical temperature (K)	392	
Critical pressure (bar)	110	

### Constant volume combustion chamber

The constant volume combustion chamber (CVCC) used in this study has a volume of approximately 1 liter, and the chamber volume geometry consists of three intersecting cylinders. The CVCC can be set up with various instruments using its ports and for this study, the CVCC was modified to work with a hollow-cone injector for liquid ammonia direct injection. Figure 2 shows the CVCC, and the injector used. The CVCC has a high-speed piezoelectric pressure transducer installed to record the changes in pressure inside the chamber. Using the heaters installed on the outside of the CVCC, we can control the temperatures of the chamber volume, this helps control the injection environment inside the CVCC precisely. An accumulator, several valves, and pressurized gas bottles were used to control the gaseous environment and pressure inside the CVCC and create an appropriate mixture of oxygen and nitrogen as needed. The exact CVCC system used in this study has been described in detail in our previous publications [19-21]. For this study, pure liquid ammonia was procured from an industrial and scientific gas supplier. The ammonia cylinder was fitted with a siphon tube to ensure the outlet provides a constant supply of liquid ammonia. From the cylinder, liquid

ammonia was measured to be between 16 and 20 bar of pressure based on the temperature of the cylinder. For initial proof of concept testing, the internal pressure of the cylinder was used without the use of any pumps to boost pressure. For further testing with elevated pressures, a custom-built pumping solution was used. The pumping system consists of an airdriven pump that uses shop-air at up to 10 bar to pump any liquid up to 3200 bar. The airdriven pump was chosen with appropriate seals and elastomers to ensure compatibility with liquid ammonia contact. The liquid ammonia when fed directly into the air-driven pump would cause the pump to vapor lock and stop pumping ammonia. This is due to the relatively low vapor pressure of ammonia causing it to vaporize in the pipe and also due to the working principle of the air-driven pump. To prevent the pump from vapor locking, a small vapor separator was designed and built in-house to ensure there is always a continuous source of liquid ammonia. The vapor separator can vent gaseous ammonia safely to maintain a consistent level of liquid to feed into the pump. Once the liquid ammonia is pressurized by the pump, it is then sent into a fuel rail that has a pressure sensor attached. This pressure sensor feeds data into the experiment control DAQ (Data Acquisition) system built using National Instruments LabView software and hardware. Based on the fuel rail pressure, the air-driven pump is controlled to maintain a stable pressure for testing. A Siemens VDO piezoelectric gasoline direct injection (GDI) outwardly opening hollow-cone injector was used for the experiments. The injector was fitted onto a plug installed on the side of the CVCC. The injector was controlled by an injector driver coupled to the NI DAQ system.

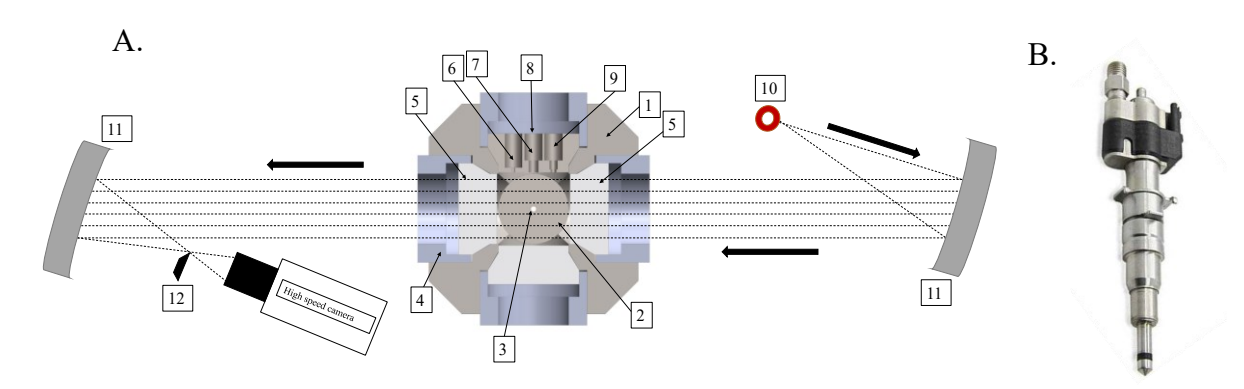


**Figure 2** A). CVCC setup — 1. Chamber body with heaters installed; 2. Combustion chamber; 3. Fuel injector location; 4. Window/Plug holder; 5. Quartz window; 6. Gas inlet port; 7. Spark plug port; 8. Exhaust port; 9. Pressure transducer port; 10. Light source; 11. Parabolic mirror; 12. Knife edge, B). Siemens VDO Piezoelectric hollow-cone injector used in this study.

## Optical diagnostic systems

Since this study focuses on the characterization of the liquid ammonia spray from a hollow-cone injector, two different techniques of high-speed imaging were employed. Backlit shadowgraph and Schlieren systems were used together to study the spray development process in detail. A Phantom VEO 710L high-speed camera was used to record the spray at frame rates up to 45000 FPS.

# **Experimental uncertainties**

The major contributions to the experimental error in this study results from the slight variations in the pressure and temperature of all the systems used. To overcome errors due to these minor uncertainties, each test case was repeated 6 times and parameters were averaged.

Overall, the experimental setup can reproduce the same spray parameters without major variations. Table 2 shows the uncertainties from the sensors used in this experimental setup.

	Table 2 Measured	uncertainties of	experimental	setup.
--	------------------	------------------	--------------	--------

Description (units)	Value	
Fuel rail pressure sensor (bar)	2	
CVCC chamber pressure (bar)	0.02	
CVCC temperature controller (K)	2.5	
Thermocouples (K)	2.5	
Air-driven high-pressure pump control (bar)	0.15	

### **Results and Discussions**

Characterization of the hollow cone spray is performed by analyzing the Schlieren high-speed images recorded. The high-speed images from the camera are firstly processed using ImageJ. and MATLAB to remove the background, crop into the region of interest, and enhance the contrast. The processed images are then used to calculate several spray parameters like spray cone angle, axial spray penetration length, spray plume width, and the spray plume ratio using a custom MATLAB code by identifying the spray edges from the images. Since the injector used in this study has been previously validated to produce an axisymmetric spray within the ranges of this study, the same is assumed in the calculations based on the spray images. Figure 3 provides a regime map of the various cases tested in this study. Figure 3 includes all the data points and combinations discussed in this study. There are 3 distinct sections indicated, they are defined based on the spray behavior at that condition. Because the injector used in this study is a hollow-cone injector, all the cases discussed below are flash boiling sprays. But, with increasing ambient temperature and injection pressure, the flash boiling spray transitions into being a supercritical spray as displayed by the suddenly increasing flash boiling intensity and changes on the spray profile. For sake of brevity, this study focuses on the effects of changing ambient temperature and injection pressure with a fixed chamber internal pressure of 1 bar.

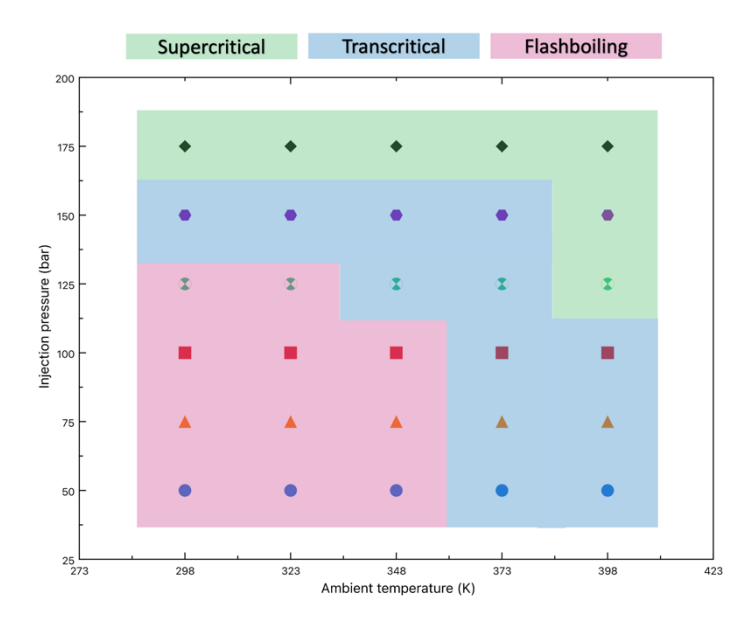
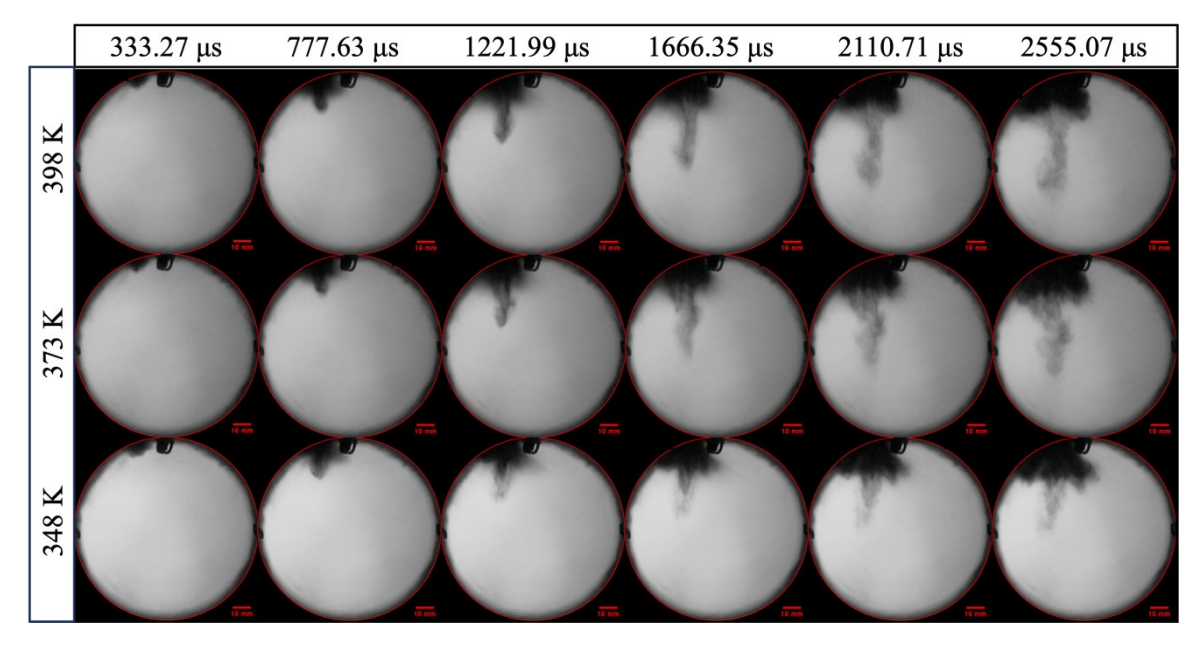


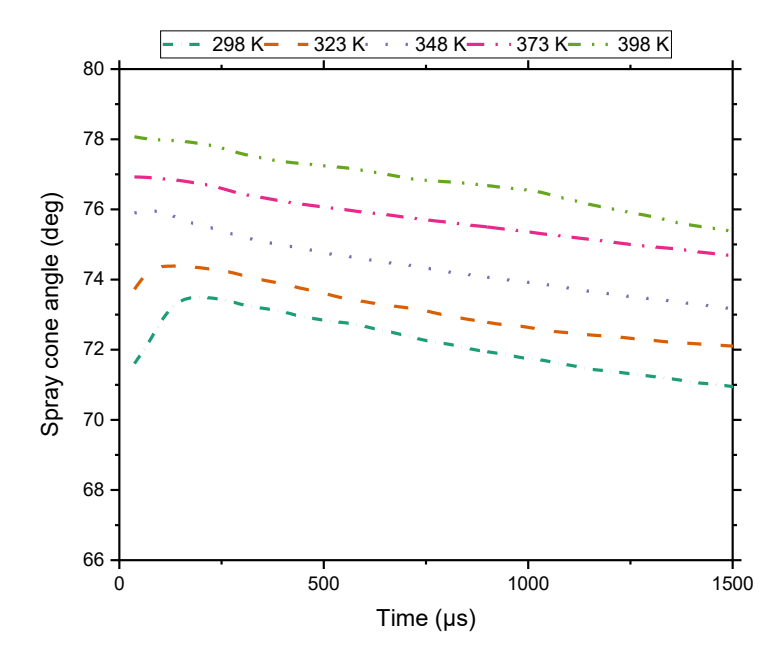
Figure 3 Regime map indicating the type of spray observed for all the cases shown in this study.

Schlieren imaging can help visualize the vaporization of the hollow-cone spray from the injector. Figure 4 shows the effect of the CVCC environment temperature on the spray development process. The three cases shown in the sequence were all injected at a pressure of 125 bar with the three columns having CVCC temperature of 348 K, 373 K, and 398 K, respectively at a chamber ambient pressure of 1 bar. Most liquefied gases like liquid ammonia tend to have high vapor saturation pressure and a lower viscosity compared to tradition liquid fuels. Hence, changes in the ambient conditions that the spray is injected into severely affect the vaporization and spray formation process. From Figure 4, we can see that the liquid ammonia spray exhibits flash-boiling for all the temperatures shown. But, with increasing ambient temperature, the intensity of flash-boiling is increased. This can be seen with the increase in the penetrating length caused by the formation of an intense central plume when the ambient temperature is changed from 348 K to 373 K. The elongation in the central plume is accelerated by the rapid flash boiling of the fuel as it exits the injector. The rapidly expanding conical liquid sheet under boiling conditions then collides with itself to forms the central plume. Moving to the next temperature of 373 K, we see that the central plump appears to be darker. This indicates that the collision of the expanding hollow-cone is more intense, resulting in a larger quantity of fuel vapor in the central plume. The spray for the 398 K case shows the spray cone to be more diffused as this could be caused by the fuel rapidly diffusing due to the conditions being favorable for ammonia to transition into a supercritical state near the injector.



**Figure 4** Sequence of high-speed images showing the effect of chamber ambient temperature for ammonia injected at 125 bar with the chamber pressure at 1 bar.

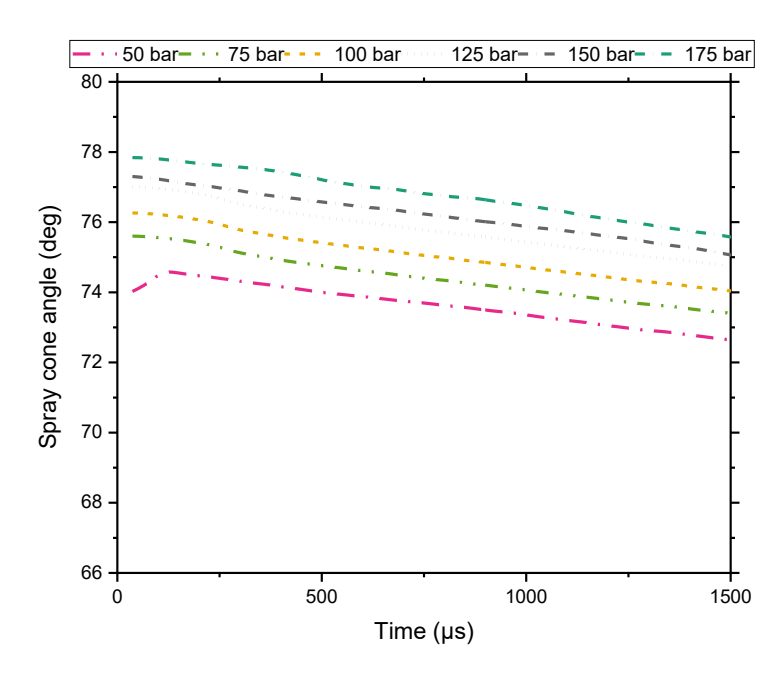
Figure 5 shows the effect of the CVCC ambient temperature on the spray cone angle of liquid NH $_3$  with an injection pressure of 125 bar and CVCC ambient pressure of 1 bar. It is evident from the data that an increase in the CVCC ambient temperature causes an increase in the flash-boiling effect, as seen by the advancement of the peak spray cone angle timing. It is also interesting to see that the transition from having a peak 235  $\mu$ s at 298 K to 94  $\mu$ s at 348 K. With higher temperatures, the peak spray cone angel is not seen, as the spray expands and diffuses rapidly. This is due to the transition into the critical regime as seen from the regime map. Even with a high fuel pressure, if the ambient temperature is low, the flash-boiling effect is lower.



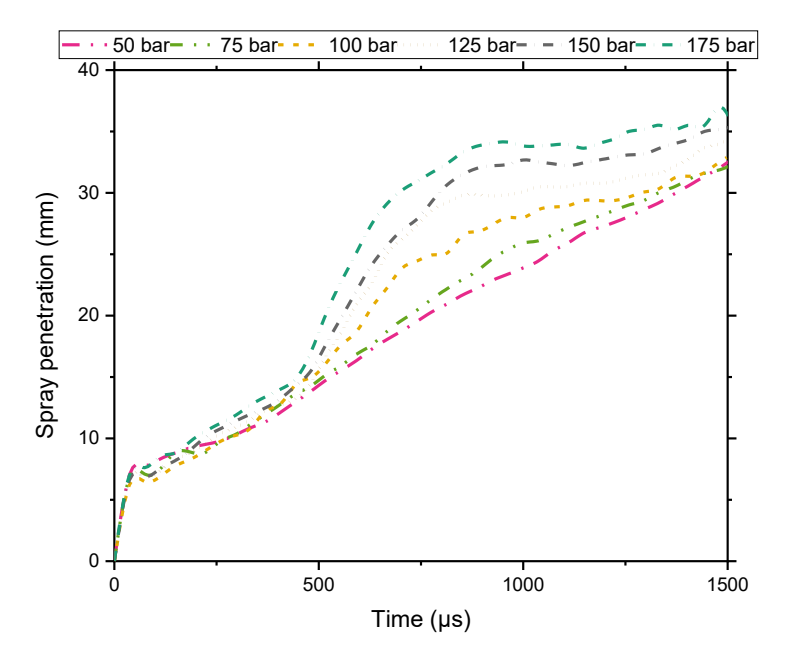
**Figure 5** Effect of chamber ambient temperature on the spray cone angle measured with a chamber pressure of 1 bar and injection pressure of 125 bar.

Figure 6 shows the effect of changing injection pressure on the spray cone angle when the fuel is sprayed at an ambient pressure of 1 bar and 373 K. For this study, injection pressure was varied from 50 bar up to 175 bar. The spray cone angle transformation over time shows a strong relationship between the injection pressure and the time to reach the peak spray cone angle. This is interesting as this can be used as an identifier for determining the intensity of flash-boiling at higher pressures. With increase in injection pressure, it is seen that there is an advancement in time to reach the peak spray cone angle. This correlates very well to the transition from being pressure and momentum-driven spray development to a transcritical, flash-boiling, and rapid vaporization dominant spray development. When increasing the pressure to above 75 bar, there is no more increase in spray cone angle with time. This indicates that NH<sub>3</sub> displays a transition into the transcritical or the supercritical regime at relatively low injection pressures compared to other fuels like ethanol and isooctane, as characterized by the rapid flash-boiling causing the formation of the central plume.

Figure 7 shows the measured axial spray penetration length with varying injection pressure with the CVCC. Ambient conditions were maintained at 1 bar and 373 K. Due to the nozzle geometry of the hollow-cone injector, the fuel tends to spray in a hollow cone, thus reducing the overall penetration length. When the injection pressure is changed, the initial penetration of the spray plume is close together for all the pressures. The only noticeable difference is that with increasing injection pressure, there is a slight reduction in the penetration length in the initial stages of the spray. This is expected, as with increasing pressure, there is increased vaporization and flash boiling of the spray caused by rapid vaporization and diffusion. When the intensity of flash boiling increases, the spray tends to spread outwards, perpendicular to the conical liquid sheet of the spray that forms the spray cone. With increasing pressure, the spray crosses a threshold, after which the central spray plume formation dominates the spray penetration length, causing a very sudden increase in the penetration length at higher injection pressures. One thing to note is that this study considers the central plume tip as the overall axial spray penetration length. If one were to ignore the central plume formed because of the colliding cone, the trend would be extremely diverse. This is because more of the spray would rapidly evaporate, and the hollow cone would expand radially rather than penetrating further away axially until a maximum cone angle is achieved.



**Figure 6** Effect of Changing injection pressure on the spray cone angle with the chamber ambient pressure and temperature set to 1 bar and 373 K.



**Figure 7** Effect of injection pressure on the axial spray penetration length measured with the chamber temperature at 373 K and chamber pressure at 1 bar.

Figure 8 shows the penetration length variation with changing the CVCC ambient temperature while holding the injection pressure at 125 bar and the ambient pressure at 1 bar. At higher CVCC ambient temperatures, the penetration of the spray is slowed due to the spray expanding conically and radially in the initial stages of the injection. This is caused by the increase in vaporization of the fuel mass. Once the central plume is formed, the penetration speed suddenly increases, causing the spray to penetrate further rapidly at higher temperatures. At higher ambient temperatures and injection pressures, once the central spray plume is formed, the axial penetration length and speed both increase rapidly. Figure 8 also

shows a non-monotonic behavior of the penetration rate with increasing temperature. Referencing the regime map in Figure 3, we can see that the fuel enters the transcritical regime with temperatures above 348 K. Looking at the penetration, we can see that there is a sudden increase in penetration rate around 500 µs after injection as the newly formed central plume is accelerated by the rapid discussion and vaporization of the fuel in the transcritical regime. When the temperature is changed to 398 K, this effect is further amplified. There is also a clear change in the early stages of the central plume formation that causes the central plume to be accelerated faster.

Figure 9 shows the calculated plume ratios of the different cases studied in the work. Using the high-speed images with the measurements of the central spray plume, the plume ratio is defined as the ratio of central spray plume radius to the overall spray cone radius. This ratio can be used as a simple way to understand the effect of flash boiling, specifically the intensity of flash boiling. If the fuel spray experiences high rates of evaporation or flash boiling, the quickly expanding cone will collide on itself radially and generate a large central spray plume. With increasing injection pressure, the plume ratio shows a steady increase as the central cone formed from the collapse of the hollow cone grows. With an increase in injection pressure, the plume ratio steadily increases. But, with change in temperature, there exists 2 regimes. With ambient temperatures at or below 348 K, the plume ratios are all grouped in a similar region. But with further increase in temperature, there is a sudden change in the ratio, suggesting that the spray has a much wider central plume. This can be caused by the increase in vaporization and diffusion as a result of the fuel transitioning into the supercritical regime.

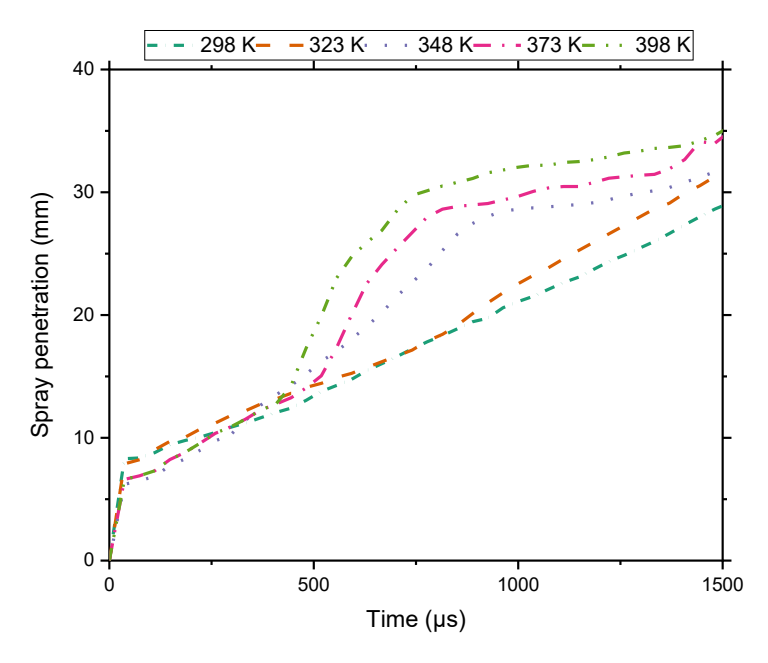


Figure 8 Effect of ambient temperatures on the axial spray penetration with the injection pressure set at 125 bar and the ambient pressure at 1 bar.

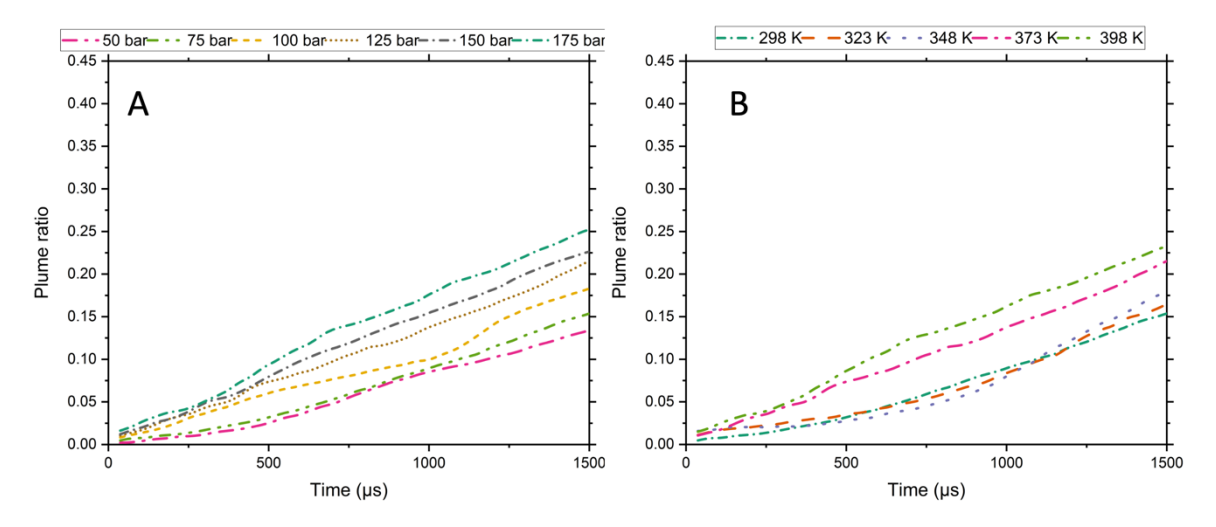


Figure 9 Plume ratios as calculated from the high-speed images, showing the effect of A), changing injection pressure, and B). changing ambient temperature.

As NH<sub>3</sub> requires a relatively high ignition energy, leveraging a spray system that can control the local equivalence ratio near a spark plug by enhancing the mixing can help improve the ignition performance in an engine [14,15,22]. Tailoring the liquid ammonia spray pattern to use the flash-boiling behavior to enhance the vaporization while still having a decent penetration length will be greatly beneficial in optimizing combustion performance.

### **Conclusions**

- By utilizing a CVCC and a piezoelectric hollow-cone GDI injector, flash boiling liquid ammonia sprays are studied to understand the spray development and transition into the critical states.
- Using high-speed imaging, the effects of changing the ambient temperature and fuel
  pressure on the flash boiling intensity and the central spray plume formation is studied,
  the spray characteristics show a clear change in behavior when transitioning through
  the transcritical regime.
- Based on the spray characteristics, a regime map has been created for liquid ammonia injections, showing the possible transition of the fuel spray into the supercritical regime.

# Acknowledgement

This material is based upon work supported by, or in part by, the National Science Foundation under Grant No. CBET- 2104394 and the CRG funding from the Clean Combustion Research Center (CCRC) of the King Abdullah University of Science and Technology (KAUST). Any opinions, findings, and conclusions or recommendations expressed in this material are those of the author(s) and do not necessarily reflect the views of the funding agencies.

# References

- [1] M. Zhang, Z. An, X. Wei, J. Wang, Z. Huang, H. Tan, Emission analysis of the CH4/NH<sub>3</sub>/air co-firing fuels in a model combustor, Fuel 291 (2021) 120135. doi:10.1016/j.fuel.2021.120135.
- [2] Hayakawa, T. Goto, R. Mimoto, Y. Arakawa, T. Kudo, H. Kobayashi, Laminar burning velocity and Markstein length of ammonia/air premixed flames at various pressures, Fuel 159 (2015) 98–106. doi:10.1016/j.fuel.2015.06.070.
- [3] A. Valera-Medina, F. Amer-Hatem, A. K. Azad, I. C. Dedoussi, M. De Joannon, R. X. Fernandes, P. Glarborg, H. Hashemi, X. He, S. Mashruk, J. McGowan, C. Mounaim-

- Rouselle, A. Ortiz-Prado, A. Ortiz-Valera, I. Rossetti, B. Shu, M. Yehia, H. Xiao, M. Costa, Review on Ammonia as a Potential Fuel: From Synthesis to Economics, Energy & Fuels 35 (9) (2021) 6964–7029. doi:10.1021/acs.energyfuels.0c03685.
- [4] H. Kobayashi, A. Hayakawa, K. K. A. Somarathne, E. C. Okafor, Science and technology of ammonia combustion, Proceedings of the Combustion Institute 37 (1) (2019) 109–133. doi:10.1016/j.proci.2018.09.029.
- [5] R. Ichimura, K. Hadi, N. Hashimoto, A. Hayakawa, H. Kobayashi, O. Fujita, Extinction limits of an ammonia/air flame propagating in a turbulent field, Fuel 246 (2019) 178–186. doi:10.1016/j.fuel.2019.02.110.
- [6] T. Cai, D. Zhao, B. Wang, J. Li, Y. Guan, NO emission and thermal performances studies on premixed ammonia-oxygen combustion in a CO2-free micro-planar combustor, Fuel 280 (2020) 118554. doi:10.1016/j.fuel.2020.118554.
- [7] Y. Niki, Y. Nitta, H. Sekiguchi, K. Hirata, Diesel Fuel Multiple Injection Effects on Emission Characteristics of Diesel Engine Mixed Ammonia Gas Into Intake Air, Journal of Engineering for Gas Turbines and Power 141 (6) (2019) 061020. doi:10.1115/1.4042507.
- [8] Y. Niki, Y. Nitta, H. Sekiguchi, K. Hirata, Diesel Fuel Multiple Injection Effects on Emission Characteristics of Diesel Engine Mixed Ammonia Gas Into Intake Air, Journal of Engineering for Gas Turbines and Power 141 (6) (2019) 061020. doi:10.1115/1.4042507.
- [9] V. Scharl, T. Lackovic, T. Sattelmayer, Characterization of ammonia spray combustion and mixture formation under high-pressure, direct injection conditions, Fuel 333 (2023) 126454. doi:10.1016/j.fuel.2022.126454.
- [10] V. Scharl, T. Sattelmayer, Ignition and combustion characteristics of diesel piloted ammonia injections, Fuel Communications 11 (2022) 100068. doi:10.1016/j.jfueco.2022.100068.
- [11] H. Guo, H. Ding, Y. Li, X. Ma, Z. Wang, H. Xu, J. Wang, Comparison of spray collapses at elevated ambient pressure and flash boiling conditions using multi-hole gasoline direct injector, Fuel 199 (2017) 125–134. doi:10.1016/j.fuel.2017.02.071.
- [12] S. Lee, Spray characteristics of alternative fuels in constant volume chamber (comparison of the spray characteristics of LPG, DME and n-dodecane), JSAE Review 22 (3) (2001) 271–276. doi:10.1016/S0389- 4304(01)00117-5.
- [13] Q. Cheng, K. Ojanen, Y. Diao, O. Kaario, M. Larmi, Dynamics of the Ammonia Spray Using High-Speed Schlieren Imaging, SAE International Journal of Advances and Current Practices in Mobility 4 (4) (2022) 1138–1153. doi:10.4271/2022-01-0053.
- [14] Z. Zhang, T. Li, R. Chen, N. Wang, Y. Wei, D. Wu, Injection characteristics and fuel-air mixing process of ammonia jets in a constant volume vessel, Fuel 304 (2021) 121408. doi:10.1016/j.fuel.2021.121408.
- [15] K. Nonavinakere Vinod, T. Fang, Experimental characterization of spark ignited ammonia combustion under elevated oxygen concentrations, Proceedings of the Combustion Institute 39 (4) (2023) 4319–4326. doi:10.1016/j.proci.2022.08.007.
- [16] J. Reiter, S.-C. Kong, Demonstration of Compression-Ignition Engine Combustion Using Ammonia in Reducing Greenhouse Gas Emissions, Energy & Fuels 22 (5) (2008) 2963–2971. doi:10.1021/ef800140f.
- [17] Y. Fang, X. Ma, Y. Zhang, Y. Li, K. Zhang, C. Jiang, Z. Wang, S. Shuai, Experimental Investigation of High-Pressure Liquid Ammonia Injection under Non- Flash Boiling and Flash Boiling Conditions, Energies 16 (6) (2023) 2843. doi:10.3390/en16062843.

- [18] Q. Xu, H. Pan, Y. Gao, X. Li, M. Xu, Investigation of two-hole flash-boiling plume-to-plume interaction and its impact on spray collapse, International Journal of Heat and Mass Transfer 138 (2019) 608–619. doi:10.1016/j.ijheatmasstransfer.2019.04.111.
- [19] L. Wang, F. Wang, T. Fang, Flash boiling hollow cone spray from a gdi injector under different conditions, International Journal of Multiphase Flow 118 (2019) 50–63.
- [20] L. Wang, K. N. Vinod, T. Fang, Effects of fuels on flash boiling spray from a gdi hollow cone piezoelectric injector, Fuel 257 (2019) 116080.
- [21] K. Nonavinakere Vinod, M. Gore, H. Liu, T. Fang, Experimental characterization of ammonia, methane, and gasoline fuel mixtures in small scale spark ignited engines, Applications in Energy and Combustion Science 16 (2023) 100205. doi:10.1016/j.jaecs.2023.100205.
- [22] Y. Niki, Y. Nitta, H. Sekiguchi, K. Hirata, Emission and Combustion Characteristics of Diesel Engine Fumigated With Ammonia, in: Volume 1: Large Bore Engines; Fuels; Advanced Combustion, American Society of Mechanical Engineers, San Diego, California, USA, 2018, p. V001T03A016. doi:10.1115/ICEF2018-9634.